Modifying the Resonances of a Xylophone Bar Using Active Control

Henri Boutin, Charles Besnainou, Jean-Dominique Polack

Acta Acustica united with Acustica
Vol. 101 (2015) 408 – 420

DOI 10.3813/AAA.918836

Modifying the Resonances of a Xylophone Bar Using Active Control

Henri Boutin, Charles Besnainou, Jean-Dominique Polack
Sorbonne Universités, UPMC Univ. Paris 06, UMR 7190, Institut d'Alembert, 11 rue de Lourmel, 75015 Paris
CNRS, UMR 7190, Institut d'Alembert, 11 rue de Lourmel, 75015 Paris, France. henri.boutin@unsw.edu.au

Summary
A simple active control method is described which extends the possibilities of a xylophone bar. It allows the performer to modify the vibration of its structure, unlike post-processing effects involving loudspeakers. These variations change the characteristics of the partials radiated by the bar. The xylophone bar, made of composite material, is equipped with two actuators and one sensor in PVDF (polyvinylidene fluoride), the mass and stiffness of which do not modify the mechanical characteristics. A controller in a feedback loop is executed on a mid-range digital signal processor. It is composed of a sum of second order band-pass filters. The selection of the controller coefficients relies on the measured transfer function between the input of the controller and the output of the sensor. First the active control method is designed to modify the resonance peaks of a simple model of a xylophone bar, whose transfer function is a superposition of three eigenmodes. Then it is applied to the real system. It is illustrated by increasing and reducing the amplitudes and/or frequencies of the first resonances, and by modifying the tuning of the xylophone bar.

PACS no. 43.40.Vn, 43.75.Kk, 43.75.Tv

1. Introduction

Hybridising musical instruments with active control offers two essential advantages to musicians: first it expands the range of sound that the instrument can produce, and then it modifies the sound radiated by the instrument itself so that the timbre does not depend on an external transmitter. For these reasons, the last 20 years have seen important advances in active musical instruments.

Early studies carried out by Besnainou [1, 2], used PID (Proportional-Integral-Derivative) control in a feedback loop to modify the vibration modes of musical instruments equipped with piezoelectric transducers. With collaborators [3, 4, 5], he changed the Helmholtz resonance characteristics of a guitar, the rocking motion of a violin bridge and the first bending modes of a xylophone bar.

Other studies have focused on the eigenmodes of vibrating strings. Berdahl and Smith [6] modified the damping of an electric guitar string using an integral controller in the feedback loop. They [7] also suggested an optimal adaptive method to control the amplitude of the string displacement, and applied it in simulation to induce new dynamics in a string model. In the Magnetic Resonator Piano, McPherson [8] used electromagnetic solenoids to change the sound level and the frequency of the first partials of each string, relative to the fundamental. The method requires only one sensor below the soundboard and a filter bank. The actuators are controlled using optical sensors which measure the position of the piano keys.

Active control methods were also applied to percussive instruments. Rollow [9] modified the first eigenmodes of a kettledrum. The membrane was equipped with four accelerometers. Four drivers were mounted in a plane parallel to that of the membrane. Their vibrations were coupled by the closed volume of air between the membrane and the drivers. The duration of the first partials were extended or shortened, using feed-forward control which assured system stability. In the *Feed-Drum*, Lupone and Seno [10] allowed the performer to modify the sustain of partials with feedback proportional control. This bass drum was only provided with one pair of transducers: a piezoceramic sensor was placed on the rim of the membrane and a loudspeaker was located below the membrane. Van Walstijn and Rebelo [11] suggested a method that modifies the sound radiated by a conga. The membrane vibration was measured using a contact microphone at one point of the surface and was driven by one loudspeaker mounted inside the instrument. In the feedback loop, an equalising filter cancelled the membrane natural resonances and added virtual resonances with desired characteristics.

In this paper, a new method is suggested which requires only one pair of piezoelectric transducers. A controller located in a feedback loop is implemented in a DSP (digital signal processor). It assigns desired frequencies and amplitudes to resonances of a vibrating structure. Unlike PID controllers, the transfer function of the controller tends to zero at low and high frequencies and the bandwidth of the

Received 05 March 2014,
accepted 06 January 2015.

resonance peaks can be modified by the performer. Thus no selective band-pass filter is required to preserve distant modes from unwanted modifications. As a result the controller has relatively low order and does not need to be run by high-speed processor: the sample frequency of the DSP is 48.8 kHz.

The suggested method is applied to the first bending modes of a xylophone bar equipped with transducers. The system is described in the next section. The position of the actuators allows modifications on odd bending modes rather than even bending modes. For this reason only the modes 1 and 3 are modified. The subsequent modes are considerably damped compared to the first three modes, so that the corresponding overtones do not significantly contribute to the radiated sound, as explained by Bork [12]. So they would require substantial modifications to change the sound of the bar, involving a power larger than the regulator and actuators could supply. In consequence the subsequent modes are kept unchanged. In Section 3, a simple model is established and the method to choose the controller coefficients is detailed. This method is illustrated and discussed in Section 4 through three experiments which show that the performer can apply independent modifications to the characteristics of the modes of the xylophone bar. The first two experiments aim at modifying successively the amplitudes and the frequencies of the modes 1 and 3 without changing the other characteristics and the nearest modes. In the third, the controller changes the tuning of the bar.

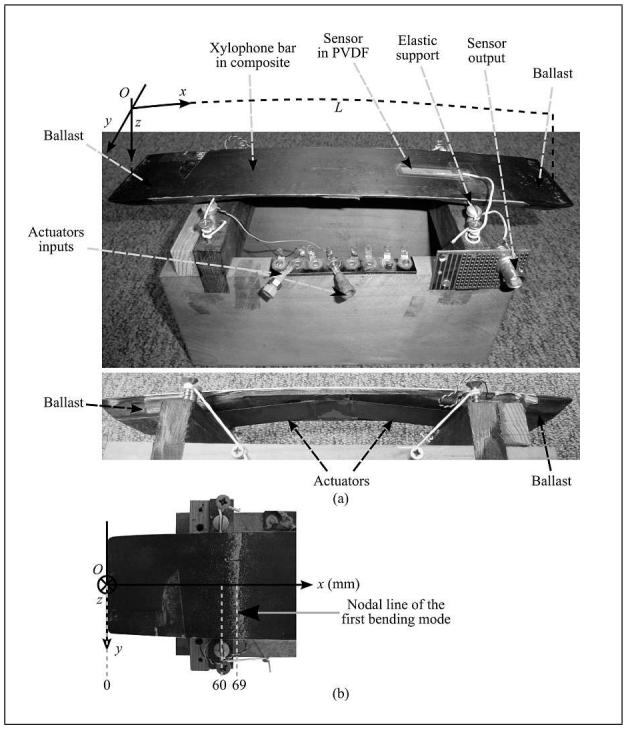

Figure 1. (a) The xylophone bar in composite equipped with transducers. (b) Close-up on the position of one elastic cord and one nodal line of the first bending mode, observed using the Chladni method. The other nodal line has a symmetric position about the middle of the bar ($x = L/2$). The third bending mode also features two nodal lines at the same positions.

2. System

2.1. Xylophone bar

The xylophone bar used in the experiment was made by the second author. The faces are of carbon fibre. The core is composed of ballasts at both extremities and of polymeric foam in the middle (Figure 1a). This composite material makes the mass at least ten times lighter than the mass of a typical xylophone bar, made of maple, spruce or tropical wood, and having the same fundamental frequency.

The length of the bar is significantly larger than its width and thickness, so that the first vibration modes are bending modes along this dimension, subsequently called x. The xylophone bar features a slight curvature of radius 1.3 m and an undercut on its lower face. Two elastic cords come across two holes drilled sideways to support the bar. The holes, located at 6 cm from each extremity of the bar, are close to the nodal lines of the first bending mode of the bar, as shown by the Chladni pattern in Figure 1b, and also to nodal lines of the third bending mode. Consequently the amplitude of these modes is little attenuated by the cords. Because of the elasticity of the cords, the boundary conditions of the bar are assumed to be free-free in first approximation like a typical xylophone bar, as suggested by Chaigne and Doutaut [13].

In a previous study, Chaigne *et al.* [14] showed that the sandwich composition of the bar and its inhomogeneity result in an unusual tuning: 1:2.7:4.9 instead of 1:3:9 or 1:4:9, while the slight curvature does not significantly affect the frequency of the partials. From Fletcher and Rossing [15], the frequency separation between the first two partials is usually adjusted by reducing the thickness at the centre of the bar. However the thickness of the xylophone bar in composite was too small to be reduced further.

2.2. Transducers

Two piezoelectric actuators made of PVDF are attached to the lower face of the bar as shown in the lower picture of Figure 1a. Each has an extremity glued at the centre and the other extremity at an edge of the undercut. The curvature of the bar reduces the angle between the actuators and the perpendicular to the bar at the fixing points, and therefore increases the bending moment applied by the actuators.

Due to the bar symmetry, the median plane $x = L/2$, L being the length of the bar, is an antinode for the odd eigenmodes, and a node for the even eigenmodes. In addition as shown by Suit's numerical model [16], the strain of the first three eigenmodes is small near the edge of the undercut. Thus the actuators location is not adapted to modify the second eigenmode, and justifies the purpose of modifying rather the first and third ones. To this end, the two actuators are supplied with the same voltage.

The xylophone bar has only one sensor, also made of PVDF, glued on the upper face of the bar. The charge difference between its faces is proportional to the strain. Thus

the ideal position to observe the first and third modes is the middle of the bar, symmetrically about the antinode line $x = L/2$. However, to not disturb the musician's performance, the sensor is moved towards one end of the bar. In order to observe the first and third bending modes, the sensor is not centred on their nodal lines, previously identified by the first author [17] using the Chladni method.

Thanks to the geometrical and mechanical characteristics of the bar and the transducers, see Table I, the voltage required by the actuators to act on the first bending modes is relatively low, around 10 V.

2.3. Feedback loop

A controller is placed in a feedback loop between the sensor and the pair of actuators. It is implemented in a DSP.

As shown in the block diagram in Figure 2, the sensor is connected to the controller via one input of the DSP, henceforth called u_1. The other input of the DSP, henceforth called u_2 is used to measure the closed-loop transfer functions. When the inputs of the DSP are connected to the output without any system in-between, the measured gain, subsequently called K_{DSP}, is 0.8 and the delay, τ_{DSP}, is equal to 287 µs and corresponds to 14 sample periods. Both characteristics are constant over a frequency range including the first three eigenmodes.

A USART (Universal Synchronous Asynchronous Receiver Transmitter) connection is set up between the DSP and a computer. It allows the user to modify the coefficients of the controller while it is running.

The output level of the DSP is limited to 3 V. It is not enough to apply audible modifications to the sound radiated by the xylophone bar. Consequently, an amplifier is inserted in the feedback loop downstream of the DSP. Its gain, equal to 75, is constant over the frequency range of interest and the phase difference between its input and its output is negligible.

3. Method

3.1. Transfer functions

In order to modify the frequency and the sustain of the first partials, the suggested method seeks a controller which assigns the desired characteristics to the resonance peaks of the system (xylophone bar and transducers). The two inputs of the system, f_h and u_{act}, are respectively the force of the mallet and the voltage supplied to the two actuators (close-up of the block diagram in Figure 2). The output y is the voltage between the faces of the sensor.

The system is thus described by two transfer functions: $G_1 = Y/F_h = H_{\text{sens}}G_{10}$ and $G_2 = Y/U_{\text{act}} = H_{\text{sens}}G_{20}H_{\text{act}}$, where F_h, U_{act} and Y are the Laplace transforms of f_h, u_{act} and y. G_{10} is the transfer function between the external force F_h and the strain of the sensor. G_{20} is the transfer function between the distributed force applied by the actuators and the strain of the sensor. H_{sens} and H_{act} are the transfer functions of the sensor and the actuators.

In the feedback loop, the DSP is composed of three blocks. One is the transfer function of the controller H_{corr} and the two other describe the gain K_{DSP} and the delay τ_{DSP} introduced in §2.3. The DSP output signal is amplified by the constant gain K_{amp} before feeding the actuators. The sensor is connected to the input u_1 of the DSP. The other input, u_2, is used in the following to measure the closed-loop transfer function in order to choose the controller characteristics and is set to 0 while the performer is playing.

The controller aims at assigning the desired characteristics to the peaks of the closed-loop transfer function G_{cl}^0,

Table I. Composition and geometry of the xylophone bar equipped with transducers.

Faces	Carbon fibre
Core	Centre: polymeric foam Extremities: ballast in polymer
Total mass	24 g
Geometry of the bar:	
Arc length	262 mm
Width	53 mm
Height	4 mm at the centre 10 mm at both extremiies
Undercut length	162 mm
Radius of curvature	1.3 m
Positions of the transducers:	
Sensor	Extremities at $x = 167$ mm and 197 mm. Width = 6 mm
Actuator 1	Extr. at $x = 50$ mm and 131 mm
Actuator 2	Extr. at $x = 131$ mm and 212 mm Width = 48 mm (both actuators)

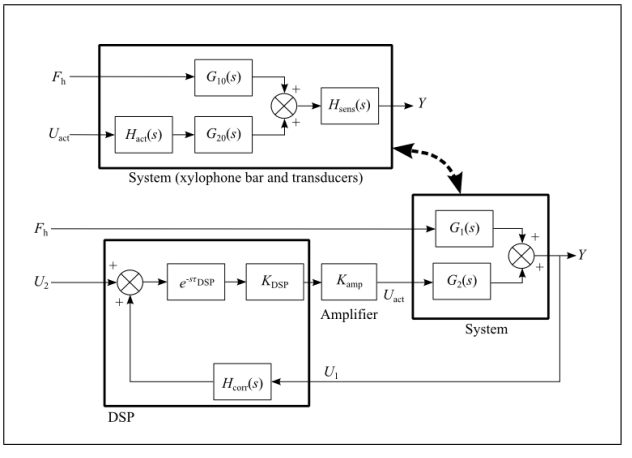

Figure 2. Block diagram of the closed-loop, composed of the system (xylophone bar and transducers), the DSP and the amplifier. s stands for Laplace variable. The two actuators are supplied with the same voltage u_{act}. The upper case variables, F_h, U_{act}, Y, U_1 and U_2 are the Laplace transforms of the time signals f_h, u_{act}, y, u_1 and u_2 previously defined. G_{10} is the transfer function between the external force F_h and the strain of the sensor faces. G_{20} is the transfer function between the distributed force applied by the actuators and the strain of the sensor. H_{sens} and H_{act} are the transfer functions of the sensor and the actuators, and G_1 and G_2 are the two transfer functions of the system (xylophone bar and transducers).

defined as the quotient Y/F_h while $U_2 = 0$ and given by the equation

$$G_{\mathrm{cl0}} = \frac{Y}{F_h}\Big|_{U_2=0} = \frac{G_1}{1 - G_2 K \mathrm{e}^{-s\tau_{\mathrm{DSP}}} H_{\mathrm{corr}}}. \qquad (1)$$

$K = K_{\mathrm{amp}} \cdot K_{\mathrm{DSP}}$ is the constant gain introduced by the DSP and the amplifier in the feedback loop. The coefficients of H_{corr} are chosen in order to apply the desired characteristics to the peaks of G_{cl0}. As shown in Equation (1), they depend on the values of the two transfer functions G_1 and $G_2 K \mathrm{e}^{-s\tau_{\mathrm{DSP}}}$. The experimental setups used to identify them are subsequently described.

3.1.1. Transfer function between the impact hammer and the sensor

In order to measure G_1, the xylophone bar is impacted by a 10 g miniature hammer (5800SL, Dytran, CA, USA). The force sensor of the hammer has a resonance frequency of 300 kHz, which is much higher than the frequencies of the considered modes. Its extremity, made of steel, has a 2.5 mm diameter allowing punctual impacts in first approximation. To make the external force repeatable, the hammer is attached to a lever which rotates on an axis parallel to the face of the bar, see Figure 3. Thanks to a horizontal stop bar, the hammer is always released from the same position without initial speed. The direction of the lever and the height of the axis are adjusted so that the hammer applies a force normal to the upper face of the bar at the impact point, on its median line $y = 0$. Thus this force essentially excites the bending modes. A rubber band attached to the horizontal stop bar damps the hammer drop, prevents bounces and makes the impact shorter.

To check how the position of the impact affects the amplitudes and frequencies of the free vibrating eigenmodes in the transfer function G_1, two measurements are carried out, by hitting the xylophone bar first at the centre (131 mm, 0 mm) and then in the position (97 mm, 0 mm). In each case, the impacts are far enough from the nodes of mode 1, as shown by the Chladni pattern in Figure 1b, and mode 3, so that both bending modes are excited. For each position, 10 impacts are applied to the bar. The hammer and sensor signals are recorded with an acquisition card (NI 9234, National Instrument, Texas, USA), sampled at 6.4 kHz and normalized, dividing the measurements by the maximum value of the hammer signal. f_h and y are the averages of these signals. The transfer functions are given by the quotient between the cross power spectrum of f_h and y, $S_{f_h,y}$ and the power spectrum of f_h, S_{f_h,f_h}. The magnitudes and phases corresponding to both impact positions are plotted in Figure 4, as well as the coherence corresponding to the central impact, defined by $|S_{f_h,y}|^2/(S_{f_h,f_h}S_{y,y})$, $S_{y,y}$ being the power spectrum of y. All subsequent transfer functions measured with this experimental setup are defined relative to the same reference 0 dB, which depends on the sensor piezoelectric constant.

When the impact is off-centre, the magnitude of G_1 (dashed black curve in Figure 4) shows three significant peaks corresponding to the first bending modes of the bar.

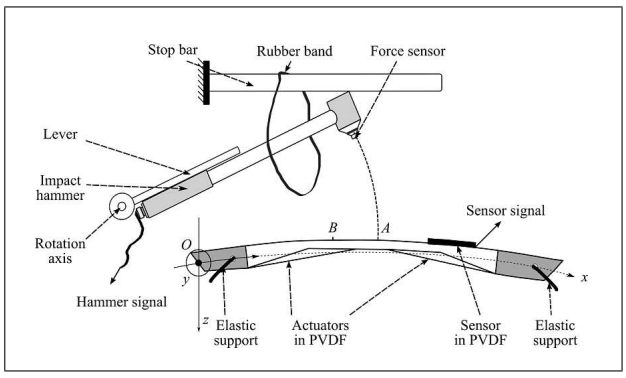

Figure 3. Experimental setup used to measure transfer functions of the xylophone bar. The impacts are applied first at the centre (131 mm, 0 mm) and then in (97 mm, 0 mm).

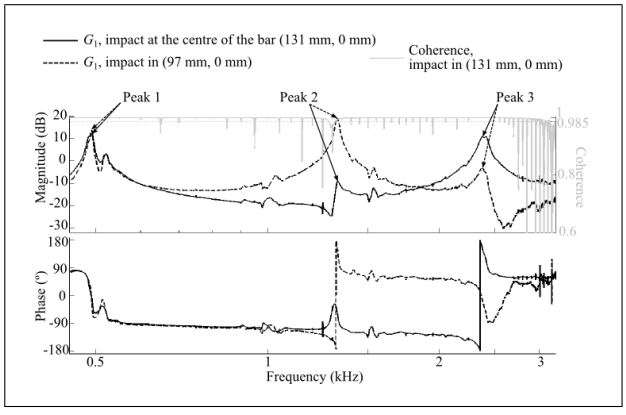

Figure 4. Magnitude (upper part) and phase (lower part) of the transfer function G_1, when an impact is applied at the centre of the bar (131 mm, 0 mm) (solid black) and off-centre (97 mm, 0 mm) (dashed black). The coherence corresponding to central impact (grey) is read on the linear axis at the right-hand side of the upper part of the figure. All curves are plotted as a function of the frequency displayed on a logarithmic scale. For each impact position, the characteristics of the peaks corresponding to the first three bending modes are given in Table II.

Table II. Characteristics of the peaks corresponding to the first three bending modes of the system (xylophone bar and transducers), for two impact positions (A: 131 mm, 0 mm) and (B: 97 mm, 0 mm). For each peak, the Q-factor Q is estimated by the quotient between the resonance frequency f_R and the bandwidth Δ at −3 dB. A: Amplitude.

		f_R	A	Q	Δ
A	Peak 1	493.3 Hz	12.4 dB	43.0	11.5 Hz
	Peak 2	1329.0 Hz	-9.0 dB	41.6	31.9 Hz
	Peak 3	2382.2 Hz	10.9 dB	24.8	95.9 Hz
B	Peak 1	492.0 Hz	13.7 dB	86.2	5.7 Hz
	Peak 2	1326.0 Hz	19.1 dB	63.4	20.9 Hz
	Peak 3	2378.0 Hz	-3.0 dB	29.6	80.4 Hz

As expected, the second peak is attenuated when the hammer hits the bar at the centre. For this measurement, the experimental setup is repeatable to measure the peaks of interest, as shown by the coherence (grey curve in Figure 4), which exceeds 0.99 over the intervals [400 Hz,

600 Hz], [1313 Hz, 1400 Hz] and [2200, 2600 Hz]. Below the second peak frequency, the coherence slightly decreases around an anti-resonance in 1.3 kHz. The other minima of coherence are multiples of 50 Hz, frequency of the mains in France.

The impact position affects the relative amplitudes of the peaks and their contribution at the frequency of the nearest peaks. In consequence, the peak frequencies in the measured transfer function are also potentially changed when the impact position is modified. However, the first three modes are well separated. Indeed the peak bandwidths at -3 dB are much smaller than the frequency separation between them. This explains why the frequency variations of the peaks are small, less than 0.3%, when the impact position is offset by 34 cm from the centre.

Another peak, located about 520 Hz, is due to the location of the actuators. Since they are not perfectly symmetric about the transversal plane $x = L/2$, they apply asymmetric prestressing to the bar, which separates the first resonance peak into two components of very close frequencies. To not damage the bar in composite, it was chosen to leave the actuators at their initial positions.

3.1.2. Open-loop transfer function in the absence of controller

The transfer function $G_2 K \mathrm{e}^{-s\tau_{\mathrm{DSP}}}$, in the denominator of Equation (1), is the open-loop transfer function when $H_{\mathrm{corr}} = 1$, see Figure 2. To measure it, a sinusoidal voltage is supplied to the input U_1 of the controller, the gain (H_{corr}) of which is temporarily set to 1. The input U_2 of the DSP is set to 0. The sensor is disconnected from the DSP. The frequency of the voltage source sweeps the range of interest [450 Hz, 3.2 kHz]. The transfer function is calculated by a spectrum analyser which simultaneously records the supply voltage and the sensor signal. The experimental setup is described by the block diagram in Figure 5a.

To measure the transfer function $G_2 K \mathrm{e}^{-2\mathrm{j}f\tau_{\mathrm{DSP}}}$ (solid curves in Figure 5b), the amplitude of the voltage source is set to 100 mV. In order to identify the range over which the system (xylophone bar and transducers) is linear, the transfer function is also measured at larger amplitudes. No modification of the transfer function is observed below 250 mV. For higher values, the amplitude of u_{act} exceeds 15 V. Then the behaviour of the actuators becomes non-linear and the measured transfer function is distorted around the first and third resonance frequencies. In the following measurements, the amplitude of the source is adjusted so that u_{act} is maintained below 15 V.

Between 600 Hz and 1300 Hz, the gain of the transfer function $G_2 K \mathrm{e}^{-2\mathrm{j}f\tau_{\mathrm{DSP}}}$ is low and has comparable level with the electronic noise in the experimental setup. Thus the precision of the phase given by the spectrum analyser over this range is significantly reduced. However around the three main peaks, the noise level is much lower than the measured gain, by more than 10 dB, so that accurate measurements of their characteristics can be achieved.

As expected, the actuators mostly excite the odd bending modes because they are supplied with the same voltage. The gains of the amplifier and DSP, and the piezoelectric constant of the actuators are included in the curves of Figure 5b, so that the characteristics of the peaks are different from those shown in Figure 4 and Table II. However the difference between the first and the third resonance frequencies of $G_2 K \mathrm{e}^{-s\tau_{\mathrm{DSP}}}$ and the ones of G_1 when the impact is applied at the centre is less than 0.5%. Thus, from Equation (1), the controller will apply approximately the same variations to the transfer functions G_{cl0} and to the transfer function G_{cl}, between the input U_2 of the DSP and the sensor signal, which is defined by

$$G_{\mathrm{cl}} = \frac{Y}{U_2}\bigg|_{F_h=0} = \frac{G_2 K \mathrm{e}^{-s\tau_{\mathrm{DSP}}}}{1 - G_2 K \mathrm{e}^{-s\tau_{\mathrm{DSP}}} H_{\mathrm{corr}}}, \qquad (2)$$

as shown by the block diagram in Figure 2. Subsequently, the controller is chosen to change the resonance characteristics of G_{cl}. To measure this transfer function, the sensor is connected to the input U_1 of the DSP, and the voltage source to the summing point in the input U_2 of the DSP. The spectrum analyser measures simultaneously the voltage source and the sensor signal and deduces the transfer function G_{cl}.

The spurious peak previously measured above the first resonance of G_1 (Figure 4) is also observed on the curve of Figure 5b, in 529.7 Hz. In section 4, the variations applied to the first peak will be restrained in order to keep unchanged the characteristics of this peak.

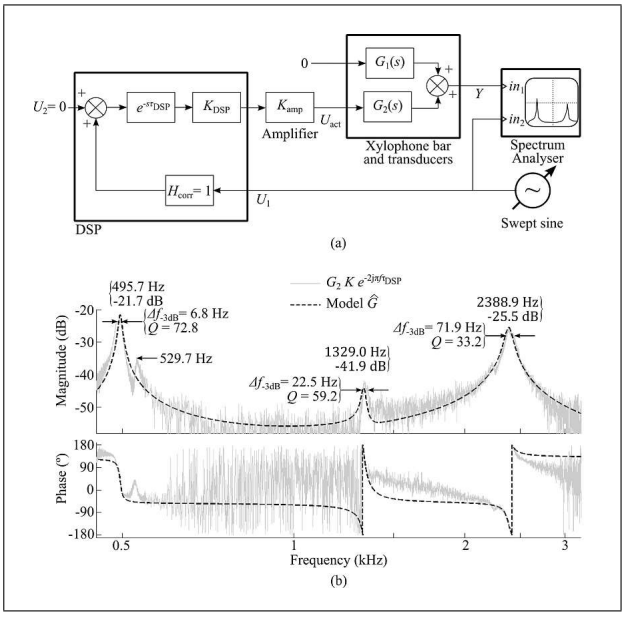

Figure 5. (a) Block diagram of the experimental setup used to measure $G_2 K \mathrm{e}^{-2\mathrm{j}f\tau_{\mathrm{DSP}}}$. (b) Comparison between the magnitudes (upper part) and the phases (lower part) of the measured transfer function $G_2 K \mathrm{e}^{-2\mathrm{j}f\tau_{\mathrm{DSP}}}$ (solid curves) and of the model $\hat{G}$ (dashed curves) described in §3.2. The curves are plotted as a function of the frequency displayed on a logarithmic scale. The frequencies, amplitudes, bandwidths at -3 dB, $\Delta f_{-3\,\mathrm{dB}}$, and Q-factors, Q, refer to the peaks of the measured transfer function $G_2 K \mathrm{e}^{-2\mathrm{j}f\tau_{\mathrm{DSP}}}$. The Q-factors are estimated by the quotient between the resonance frequencies and the bandwidths at -3 dB.

3.2. Model

In order to discuss the method to choose H_{corr} and the influence of its coefficients on the closed-loop transfer function, the controller is first applied to a model of the system (xylophone bar and transducers). Since the xylophone bar has complex geometry and inhomogeneous structure, the model is described by its eigenmodes rather than its physical properties. Its transfer function $\hat{G}$ is a sum of three second-order band-pass resonant filters $\hat{G}_k$, corresponding to the first three bending modes of the bar. Each filter $\hat{G}_k$ is characterized by four coefficients: $G_{\max_k}$, f_k, Q_k and φ_k,

$$\hat{G} = \sum_{1\le k\le 3} \hat{G}_k, \tag{3}$$

with

$$\hat{G}_k(\mathrm{j}\omega) = \frac{\frac{\mathrm{j}\omega}{2\pi f_k Q_k} G_{\max_k}}{1 + \frac{\mathrm{j}\omega}{2\pi f_k Q_k} + \left(\frac{\mathrm{j}\omega}{2\pi f_k}\right)^2} \mathrm{e}^{\mathrm{j}\varphi_{ck}}, \quad 1 \le k \le 3. \tag{4}$$

The coefficients $G_{\max_k}$, f_k and Q_k are identified to the amplitude, frequency and Q-factor of the kth peak of $G_2 K \mathrm{e}^{-s\tau_{\text{DSP}}}$ and φ_k is identified to its phase in f_k. Magnitude and phase of $\hat{G}$ are plotted in Figure 5b (dashed curves) and compared to $G_2 K \mathrm{e}^{-s\tau_{\text{DSP}}}$. Since the frequency separations between the peaks of resonance are much larger than their bandwidths at -3 dB, the first and third peaks of the model and the ones of the real system have comparable characteristics: their amplitudes, frequencies and bandwidths differ by less than 0.01 dB, 0.2 Hz and 0.2 Hz respectively. The second resonance peak of $G_2 K \mathrm{e}^{-s\tau_{\text{DSP}}}$ is relatively smaller. In consequence the differences between its characteristics and the ones of the model are larger: 2.1 dB, 1.0 Hz and 2.1 Hz. Since this peak is not modified by the controller, these differences have no consequences on the choice of its coefficients

3.3. Controller

In this section, the method to determine the coefficients of the controller is described, in order to apply the desired variations to the peaks of the model transfer function. In the vicinity of the kth resonance frequency, $k \in \{1, 3\}$, $\hat{G}$ is approximately equal to $\hat{G}_k$ since the contribution of the nearest filters is negligible (less than 46 dB smaller). A second-order band-pass resonant filter is designed to apply to the peak the desired variations of amplitude and frequency. Its transfer function H_k is specified by its resonance frequency f_{ck}, its quality factor Q_{ck}, its maximum gain $H_{\max_k}$ and its phase φ_{ck} at the frequency f_{ck},

$$H_k(\mathrm{j}\omega) = \frac{\frac{\mathrm{j}\omega}{2\pi f_{ck} Q_{ck}} H_{\max_k}}{1 + \frac{\mathrm{j}\omega}{2\pi f_{ck} Q_{ck}} + \left(\frac{\mathrm{j}\omega}{2\pi f_{ck}}\right)^2} \mathrm{e}^{\mathrm{j}\varphi_{ck}}, \quad k \in \{1, 3\}. \tag{5}$$

The controller H_{corr} is the sum of the filters H_k. For each filter, the Q-factor is set to a large enough value such that the gain $|H_k|$ is negligible compared to $|\hat{G}|$ at the nearest resonance frequencies. Thus, in the vicinity of the resonance frequency f_{ck} of H_k, the closed-loop transfer function is

$$\hat{G}_{\text{cl}} = \hat{G}\big/\big(1 - \hat{G} H_{\text{corr}}\big) \approx \frac{\hat{G}_k}{1 - \hat{G}_k H_k} \tag{6}$$

The coefficients of H_k are chosen through the four following steps:

I – **the resonance frequency** f_{ck} is set to the desired frequency of peak k;

II – **the phase** φ_{ck} is chosen to cancel the phase of the open-loop transfer function $\hat{G}_k H_k$ at the desired frequency f_{ck}:

$$\varphi_{ck} = -2n_k\pi - \arg\big(\hat{G}_k(2\mathrm{j}\pi f_{ck}\big), \tag{7}$$

where n_k is the smallest integer such that $\varphi_{ck} \le 0$. Thus, from Equation (6), at the desired frequency f_{ck}, the denominator of $\hat{G}_{\text{cl}}$ is $1 - |\hat{G}_k| H_{\max_k}$. Its value is real and can be adjusted by the value of $H_{\max_k}$.

III – **the coefficient** $H_{\max_k}$. From the expression of the denominator of $\hat{G}_{\text{cl}}$, see Equation (6), if $H_{\max_k}$ grows from zero, the closed-loop gain in f_{ck} also rises, and tends to $+\infty$ when $H_{\max_k} = 1/|\hat{G}_k|$. If $H_{\max_k}$ decreases from zero, then the closed-loop transfer function is also reduced and tends to 0 when $H_{\max_k}$ tends to $-\infty$. From Equation (6), the value

$$H_{\max_k} = \frac{1}{|\hat{G}_k(2\mathrm{j}\pi f_{ck}|} \left(1 - \frac{|\hat{G}_k(2\mathrm{j}\pi f_{ck}|}{G_{\max_k}}\right)$$

assigns the desired amplitude $G_{\max_k}$ at the desired frequency f_{ck}.

IV – **the Q-factor** Q_{ck} allows bandwidth modifications of peak k. The influence of this coefficient on the closed-loop transfer function is discussed in the next paragraphs while the controller aims at modifying the amplitude of the first peak (Figure 6) and its frequency (Figure 7).

For a positive amplitude variation of the closed-loop peak, as Q_{c1} rises, the bandwidth of the peak decreases, as shown by vertical lines in the right part of Figure 6a. In contrast, for a reduction of amplitude of the peak (left part of Figure 6a) the bandwidth increases as Q_{c1} rises.

Large values of Q_{c1} also reduce undesired effects produced by large modifications of amplitude. Indeed raising $|H_{\max_1}|$ increases the gain of filter H_1 and the variations it applies to the nearest peaks. These unwanted modifications are reduced by decreasing the bandwidth of H_1 i.e. by raising Q_{c1}. However, as described above, such a modification affects in turn the peak bandwidth.

Furthermore, when the controller reduces the peak amplitude, the gain $|\hat{G}_{\text{cl}}|$ has a local minimum in f_{c1} when Q_{c1} exceeds a limiting value. The white contour (top left corner of Figures 6a, 6b and 6c) gives this value in function of the amplitude variation. For larger Q_{c1}, the local maxima of $|\hat{G}_{\text{cl}}|$ are moved away from the desired position, involving errors in amplitude and frequency. In contrast, while the controller gives a maximum in f_{c1}, i.e. below the contour, the amplitude and frequency of the peak reach the

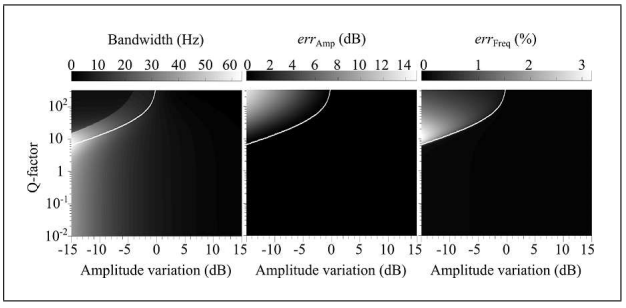

Figure 6. Influence of the Q-factor of the first filter of the controller on the bandwidth (a), the amplitude (b) and the frequency (c) of the first peak in the closed-loop transfer function $\hat{G}_{cl}$. The controller aims at modifying the amplitude of the first peak, located in 495.7 Hz without changing its frequency. $\mathrm{err}_{\mathrm{Amp}}$ is the difference (in dB) between the measured peak amplitude and the expected value, and $\mathrm{err}_{\mathrm{Freq}}$ is the relative error (in %) between the measured peak frequency and the expected value. Above the white contour, $|\hat{G}_{cl}|$ has a local minimum at the desired frequency.

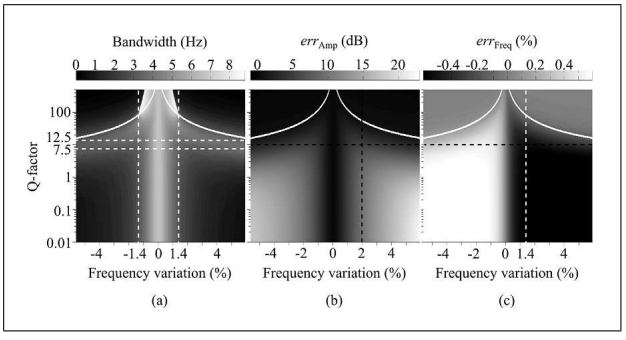

Figure 7. Influence of the Q-factor of the first filter of the controller on the bandwidth (a), the amplitude (b) and the frequency (c) of the first peak in the closed-loop transfer function $\hat{G}_{cl}$. The controller aims at modifying the frequency of the first peak, located in 495.7 Hz without changing its amplitude. $\mathrm{err}_{\mathrm{Amp}}$ is the difference (in dB) between the measured peak amplitude and the expected value, and $\mathrm{err}_{\mathrm{Freq}}$ is the relative error (in %) between the measured peak frequency and the expected value. For a Q-factor between 7.5 and 12.5, the bandwidth of the peak is larger than 3 Hz. When its value is 10, the amplitude error is maximal when the frequency variation Δf_1 is equal to 2%, and the frequency error $|\mathrm{err}_{\mathrm{Freq}}|$ is maximal when $\Delta f_1 = 1.4\%$, see dashed lines in (b) and (c). The white contour shows the threshold above which $|\hat{G}_{cl}|$ has another local maximum around the initial peak frequency.

desired values without significant errors (Figures 6b and 6c).

In the case of modification of frequency, the peak bandwidth decreases as the desired variation rises, as shown by horizontal lines in Figure 7a. However, for a given variation of frequency, see vertical lines in Figure 7a, when Q_{c1} increases, $|\hat{G}_{cl}|$ is modified on a narrower frequency range and is less attenuated around the initial frequency of the peak. Thus the bandwidth of the resonance peak of $\hat{G}_{cl}$ includes a broader interval of frequency.

As Q_{c1} rises further, the modification undergone by $|\hat{G}_{cl}|$ on either side of the initial peak is not significant. Thus $|\hat{G}_{cl}|$ has a local maximum close to the initial peak frequency, another close to the desired frequency, and a local minimum between them. This feature is observed in the top right and left corners of Figures 7a, 7b and 7c limited by white contours. Then the bandwidth of the peak is reduced again. As shown in Figure 7a, while the absolute value of frequency variation, $|\Delta f_1|$, is larger than 1.4%, the bandwidth reaches a maximum value when Q_{c1} is between 7, when $\Delta f_1 = \pm 6\%$, and 62, when $\Delta f_1 = \pm 1.4\%$. The bandwidth remains larger than 3 Hz when Q_{c1} is between 7.5 and 12.5 (region between horizontal dashed lines in Figure 7a). For frequency variations lower than 0.3%, the bandwidth is little affected by the controller and its value, greater than 6 Hz, is closer to its value in open-loop, equal to 6.8 Hz.

In the areas above the white contours, when the desired frequency moves away from its initial value, the amplitude of the local minimum between the initial and the desired peak decreases. In particular, the difference of amplitude between this minimum and the desired peak exceeds 3 dB when $|\Delta f_1|$ passes from $\pm 0.8\%$ to $\pm 1.3\%$. Thus the measured bandwidth is reduced. This explains the sudden transition observed in horizontal lines in the top part of Figure 7a.

Figures 7b and 7c show the amplitude and frequency errors, $\mathrm{err}_{\mathrm{Amp}}$ (in dB) and $\mathrm{err}_{\mathrm{Freq}}$ (in %), as the desired frequency is modified. While Q_{c1} is below 500, the amplitude variation of the peak is always larger than -0.7 dB. When the initial peak is not a local maximum of $|\hat{G}_{cl}|$, i.e. below the white contours, the errors increase as the frequency variation $|\Delta f_k|$ rises, see horizontal lines. Interestingly, when Q_{c1} is greater than 1.3, both amplitude and frequency errors reach a maximum and then slightly decrease when the frequency variation is further increased. As an example, when $Q_{c1} = 10$, the maximal errors are 5.3 dB for $\mathrm{err}_{\mathrm{Amp}}$ and 0.53% for $|\mathrm{err}_{\mathrm{Freq}}|$, and they are obtained when $\Delta f_{c1} = 2\%$ for $\mathrm{err}_{\mathrm{Amp}}$, and when $\Delta f_{c1} = 1.4\%$ for $|\mathrm{err}_{\mathrm{Freq}}|$ (see intersection between dashed lines in Figures 7b and 7c).

To illustrate the influence of Q_{c1}, the closed-loop transfer function is calculated, with controllers designed to modify the amplitude of the first peak (Figure 8a) and its frequency (Figure 8b). H_{Amp1} and H'_{Amp1} aim at increasing the amplitude of the first peak by 15 dB without changing its frequency. The only difference between these controllers is their Q-factor, equal to 3 and 100 respectively. They apply the desired variation with no significant error of amplitude and frequency. However, in agreement with Figure 6a, H'_{Amp1} gives a narrower peak than H_{Amp1}, see dark grey curves of Figure 8a.

Controllers H_{Amp2}, H'_{Amp2} and H''_{Amp2} aim at reducing the peak amplitude by 15 dB without changing its frequency. Their only difference is the value of their Q-factors: $Q_{c1} = 3$ for H_{Amp2}, 0.001 for H'_{Amp2} and 20 for H''_{Amp2}. As shown by the solid and dashed pale curves of Figure 8a, the bandwidth of the peak gets wider when the Q-factor of the controller increases from 0.001 to 3. However for the highest value $Q_{c1} = 20$, the peak is turned into a local minimum, see black dotted curve.

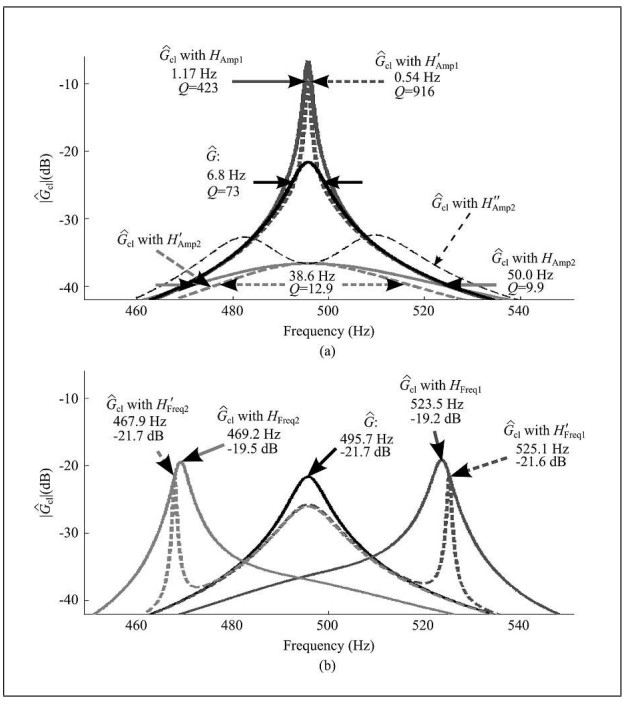

Figure 8. (a) Transfer functions $\hat{G}$ (solid black) and of the closed-loop model $\hat{G}_{cl}$ with controllers designed to modify the peak amplitude without changing its frequency: H_{Amp1} (solid dark grey) and H'_{Amp1} (dashed dark grey) aim at increasing the amplitude by 15 dB and only differ by their Q-factor, equal to 3 and 100 respectively. H_{Amp2} (solid pale grey), H'_{Amp2} (dashed pale grey) and H''_{Amp2} (dashed black) aim at decreasing the amplitude by 15 dB and only differ by their Q-factor, equal to 3, 0.001 and 20 respectively. (b) Transfer functions $\hat{G}$ (solid black) and $\hat{G}_{cl}$ with controllers designed to modify the peak frequency without changing its amplitude: (solid dark grey) and (dashed dark grey) aim at increasing the frequency by 1 semi-tone. H_{Freq2} (solid pale grey), H'_{Freq2} (dashed pale grey) aim at decreasing the frequency by 1 semi-tone. H'_{Freq1} and H'_{Freq2} differ from H_{Freq1} and H_{Freq2} only by their Q-factors, equal to 100 and 10 respectively. For each controller, the amplitude and the frequency of the peak of $\hat{G}_{cl}$ are written on the curve.

With H_{Amp2} and H'_{Amp2}, the amplitudes of the first peak of $\hat{G}_{cl}$ are equal to the desired value and their frequencies are moved by less than 0.06%. For larger reduction of amplitude, the contribution of subsequent peaks at the desired frequency f_{c1} has more impact on the characteristics of the peaks and introduces greater errors. With H''_{Amp2}, since the two maxima of $\hat{G}_{cl}$ are moved away from the desired characteristics, the errors in amplitude and frequency are significant: $\text{err}_{Amp} \geq 3.9$ dB and $\text{err}_{Freq} \geq 2.7\%$.

H_{Freq1} and H_{Freq2} aim at modifying the frequency of the first peak of $\hat{G}_{cl}$ by +5.9% (+1 semi-tone) and −5.6% (−1 semi-tone) respectively without changing its amplitude, see solid curves of Figure 8b. Their Q-factors are set to 10. H'_{Freq1} and H'_{Freq2} differ from H_{Freq1} and H_{Freq2} only by their Q-factors, equal to 100. With these controllers, the errors of frequency and amplitude are reduced to 0% and less than 0.1 dB respectively. However the peak bandwidth is also significantly reduced and the closed-loop transfer function has another maximum near the initial frequency, as shown by the dashed curves of Figure 8b. These observations are consistent with the results given in Figure 7.

3.4. Stability

From Equation (6) the stability of the model depends on the roots of the polynomial $D-N$, where N and D are the numerator and the denominator of the open-loop transfer function $\hat{G}H_{corr}$. Since $\hat{G}$ is a superposition of three eigenmodes and H_{corr} is composed of two second-order bandpass filters, D is a polynomial of degree 10. In general the constant delay introduced by the DSP and the controller coefficients φ_{ck}, $k \in \{1,3\}$ add a non-zero phase to the open-loop transfer function, which cancels only at the desired frequencies f_{ck}. Consequently, the polynomial N has complex coefficients. Hwang and Tripathi [18] show that the polynomial $|D-N|^2$ has real coefficients, the same zeroes as $D-N$ and twice its degree i.e. 20. Then to investigate the closed-loop stability, the Routh-Hurwitz criterion is applied to $|D-N|^2$. The 20 resulting inequations give sufficient conditions of stability on the eight controller coefficients. In general, each condition depends on several coefficients multiplying each other and raised to different powers between 0 and 20. In consequence no analytic solution can be found. Suitable coefficients can still be deduced from testing the system of inequations for a large range of values.

Additional assumptions specific to the current model make the resolution easier. Indeed in the open-loop transfer function, since the distance between the peaks is much larger than their bandwidth, around f_{ck}, the contribution of the nearest peaks is negligible. Therefore, in first approximation, the poles of $\hat{G}_{cl}$ are the zeroes of $1-\hat{G}_k H_k$, $k \in \{1,3\}$, i.e. the zeroes of $D_k - N_k$, N_k and D_k, being the numerator and the denominator of $\hat{G}_k H_k$. Then the Routh-Hurwitz criterion, subsequently applied to both 8th degree polynomials $|D_1 - N_1|^2$ and $|D_3 - N_3|^2$, gives two independent systems of eight inequations each. Their resolution is faster than the previous one.

We study the system stability in a simple case, where the controller modifies the amplitude of the first peak but not its frequency. The controller is composed of only one filter. Its resonance frequency is $f_1 = 495.7$ Hz and its phase coefficient is given by Equation (7). The stability conditions were tested by varying Q_{c1} and H_{max1}, in the ranges $[0.01, 1000]$ and $[-1000, 1000]$ respectively, with a step of 0.01. The closed-loop system is stable for all tested values of Q_{c1}, and for $H_{max_1} < 12.12$. This limiting value is equal to $1/G_{max_1}$ and makes $\hat{G}_{cl}$ tend to $+\infty$ at the frequency f_1. This is in agreement with Equation (6).

4. Application to the xylophone bar

The method previously described is illustrated by applying three different modifications to the first and third modes of the real system (xylophone bar and transducers).

4.1. Preliminary steps

4.1.1. Determining the controller

In practice the controller has the same design as the one used to control the model. It is a sum of two second-order band-pass filters H_1 and H_3 associated to the first and third bending modes of the system. They are defined by Equation (5). For each filter, the coefficients are chosen through four experimental steps.

I – **the resonance frequency** f_{ck} is set to the desired frequency.

II – **the phase coefficient** φ_{ck} is chosen to make the open-loop transfer function real at the frequency f_{ck}. Thus the denominator of G_{cl}, given by Equation (2), is also real:

$$1 - G_2 K \mathrm{e}^{-2\mathrm{j}\pi f_{ck}\tau_{\mathrm{DSP}}} H_{\mathrm{corr}} \approx 1 - |G_2| K H_{\mathrm{max}_k}, \qquad (8)$$

and its value is adjusted by H_{max_k}.

The experimental setup used to find the phase coefficient is shown in Figure 5a. The external voltage U_2 and the force F_h are equal to zero. A swept sinusoidal voltage is applied at the input U_1 of the DSP, connected to the controller. The open-loop transfer function $G_2 K \mathrm{e}^{-2\mathrm{j}\pi f \tau_{\mathrm{DSP}}} H_{\mathrm{corr}}$ is given by the spectrum analyser, which measures both the voltage source and the sensor output. H_{max_k} is temporarily set to 1. The value of Q_{ck} should be large enough to make the bandwidths of H_1 and H_3 much smaller than the frequency separations $f_2 - f_1 = 833\,\mathrm{Hz}$ and $f_3 - f_2 = 1060\,\mathrm{Hz}$, as shown in Figure 5b, so that the gains $|H_k|$ have no significant influence on the nearest peaks. Also Q_{ck} should be kept as small as possible for two reasons mentioned in §3.3.IV:

- to prevent the resonance peak from becoming a local minimum when its amplitude is reduced,
- to attenuate the amplitude of the initial peak as much as possible when its frequency is modified.

In practice Q_{ck} is typically set to 10, so that the bandwidths of H_1 and H_3 are approximately 50 Hz and 240 Hz.

Then the phase coefficient is adjusted to set the phase of the measured transfer function in f_{ck} to 0°, as suggested by Equation (7).

In practice, the samples at the output of the DSP are stored in a buffer. Then the phase coefficient is approximated by $2\pi f_{ck} N_s / F_s$, N_s being the length of the buffer and F_s the sample rate of the DSP. Thus, the maximal error of phase, $\pi f_{ck}/F_s$, is proportional to the desired frequency f_{ck}.

III – **The coefficient** H_{max_k} is deduced from the measurement of the closed-loop transfer function G_{cl}. It is measured using the experimental setup shown in Figure 2: the sensor output Y is connected to the input U_1 of the DSP and a sweeping voltage source is applied to the summing point, at the input U_2 of the DSP. G_{cl} is given by the spectrum analyser which simultaneously measures the voltage source in U_2 and the sensor signal Y. Then H_{max_k} is set to zero and is increased in absolute value until G_{cl} reaches the desired amplitude at the frequency f_{ck}.

IV – **The Q-factor** Q_{ck}. As explained in §3.3.IV, for large variations of amplitude, the value Q_{ck} is raised in order to reduce the gain $|H_k|$ at the frequencies of the nearest peaks. However Q_{ck} must remain below a limiting value to prevent unwanted variations of bandwidth on the considered peak.

Table III. Coefficients of controllers designed to apply amplitude variations of −10 dB, −5 dB, +5 dB and +10 dB to peaks 1 and 3. N_{s1} and N_{s3} are the buffers' lengths associated to the filters H_1 and H_3. They set the phase coefficients of the controllers.

		−10 dB	−5 dB	+5 dB	+10 dB
H_1	H_{max_1}	-51	-17	12	21
	f_{c1}	495.7	495.7	495.7	495.7
	Q_{c1}	4	4	100	100
	N_{s1}	37	37	37	37
H_3	H_{max_3}	-28	-6	7	11
	f_{c3}	2388.9	2388.9	2388.9	2388.9
	Q_{c3}	4	4	100	100
	N_{s3}	13	13	13	13

4.1.2. Calibration

In the real system (xylophone bar and transducers), the performer selects ranges of values which guarantee the system stability through a user-created preset. It involves increasing the coefficient H_{max_k} of each filter from zero, so that the gain of the closed-loop transfer function at the desired resonance frequencies rises and the damping of the partials in the radiated sound decreases. As mentioned in §3.3.III, when the coefficient H_{max_k} tends to $1/|\hat{G}_k|$, the amplitude of the closed-loop transfer function tends to $+\infty$ at the desired frequency f_{ck}. Then the oscillation of the bar starts to diverge, the amplitude of the strain reaches a limit, and non-harmonic modes are excited. This extreme situation does not cause any damage on the xylophone bar, because the power of the actuators is too low. Before reaching this nonlinear behaviour, the bar passes through a self-oscillating state that can be of musical interest for the performer.

Thus the calibration step allows performers to impose an upper limit to coefficients H_{max_k} corresponding to the minimum damping desired for each partial of the sound.

4.2. Modifications of amplitudes

The first experiment aims at applying the same amplitude variations to the first and third peaks of G_{cl}, defined as the closed-loop transfer function between the input U_2 of the DSP and the sensor signal Y, without changing the resonance frequencies. Four controllers are determined to reduce their amplitude by 10 dB and 5 dB and then to increase them by 5 dB and 10 dB. For each controller, the coefficients of the filters H_1 and H_3 are shown in Table III.

The values of f_{ck} are the frequencies of peaks 1 and 3 measured on Figure 5b. As expected, the coefficients H_{max_k} are negative for amplitude reductions and positive for increases and they rise as the desired variation grows. For both reductions, the Q-factor is reduced from its initial value, equal to 10, in order to decrease the closed-loop

gain on both sides of the peaks. On the contrary when the peaks are increased, the Q-factor is raised so that the peaks 1 and 3 are increased over a narrower bandwidth and the nearest peaks are unchanged.

The delay is given by the length of the buffer which collects samples at the DSP output. For each controller, its value is the same because changing $H_{\max_k}$ does not modify the phase of the filter in f_{ck}. The closed-loop transfer functions, G_{cl} (Figures 9a and 9b) were measured around both considered peaks using a spectrum analyser and a sinusoidal voltage source connected in the input U_2 of the DSP, as shown in the setup in Figure 2. The electronic noise due to the experimental setup was reduced in the measured curves using a Savitzky-Golay smoothing filter of order 25 [19]. Thus the curves are readily compared to the closed-loop transfer function G_{cl0}, measured between the force of the impact hammer and the sensor signal, and averaged over 10 recordings, as described below. The smoothing filter does not change the frequency and the amplitude of the peaks significantly. Indeed in the absence of controller the measured peaks 1 and 3 (black curve in Figure 9) are modified by less than 0.06% (1 cent) in frequency and 0.4 dB in amplitude compared to the values measured in Figure 5b.

With the controllers, the frequency of peak 1 appears to be modified by less than 0.1% compared to its initial value. When the amplitude of peak 3 is increased, its frequency variation is less than 0.08%. It reaches larger values, up to 0.99% (16.5 cents), when the controller aims at reducing its amplitude by 10 dB. Indeed as the frequency moves away from f_{c3}, the controller gain decreases. Then the amplitude reduction caused by the controller also decreases. In consequence for substantial reductions of the peak, the closed-loop gain has a local minimum close to f_{c3} and the local maximum is significantly moved when the desired reduction is −10 dB. Controllers with smaller Q-factor reduce this effect but also increase the modifications of the nearest peaks of G_{cl}.

In each experiment, the differences between the measured amplitudes and the desired values are less than 0.5 dB. Smaller differences are achieved with a more accurate adjustment of the coefficients $H_{\max_k}$.

We measure the modifications applied by each controller to the peaks of $G_{\mathrm{cl0}} = Y/F_h|_{U_2=0}$, where Y and F_h are the Laplace transforms of the sensor signal and the hammer force and U_2 is the DSP input connected to the summing point. The experimental setup is described in §3.1.1. We apply 10 impacts at the centre of the bar which is a node for the second mode. Thus the second peak of G_{cl0} has a small amplitude and its variation caused by the controllers does not affect the characteristics of the first and third peaks. Consequently the variations of these peaks can be compared with the variations previously measured on the peaks of G_{cl}. The transfer function G_{cl0} is given by the quotient $S_{f_h,y}/S_{f_h,f_h}$, where y and f_h are the averages over 10 recordings of the sensor signal and the hammer force, and $S_{x,y}$ denotes the cross power spectrum of x and y. The transfer functions around the peaks 1 and 3 are shown in Figures 9c and 9d.

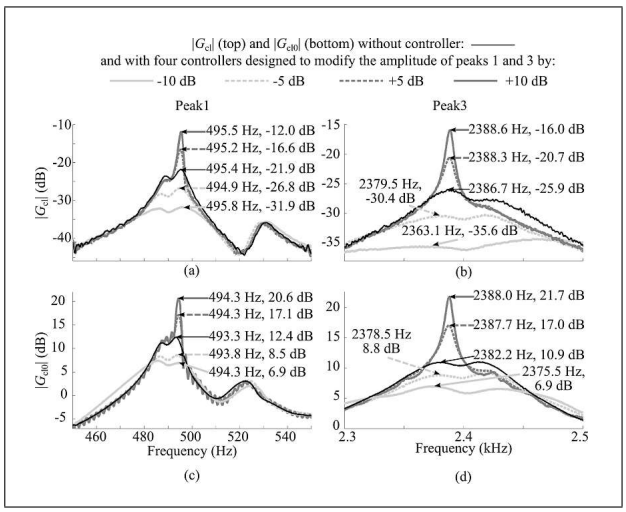

Figure 9. Closed-loop transfer functions G_{cl}, (a) and (b) and G_{cl0}, (c) and (d) measured with four different controllers designed to apply amplitude variations of −10 dB, −5 dB, +5 dB and +10 dB to the first peak, (a) and (c), and to the third peak, (b) and (d). The rest of the transfer function (not shown in the figure) is not modified.

The frequency of peaks 1 and 3 differ from their initial values by less than 0.3%. These variations have the same order of magnitude as the discrimination threshold of human hearing, estimated at 0.2% by Fastl and Zwicker [20].

The measured variations of amplitude are smaller than the desired values because the peak locations of $G_{\mathrm{cl}} = Y/U_2|_{F_h=0}$ are slightly different from the ones of $G_{\mathrm{cl0}} = Y/F_h|_{U_2=0}$. Then, at the peak frequencies, the gains of the controllers differ from the values needed to apply the desired correction. Again, decreasing the Q-factors Q_{ck} reduces these errors but also modifies the characteristics of the nearest peaks.

As a result, the controllers apply desired amplitude variations, between −10 dB and +10 dB, to the first and third resonance peaks of the system (xylophone bar and transducers) simultaneously with relative frequency variations smaller than 1%. When the bar is impacted at its centre by a hammer, the amplitudes of the free vibrating eigenmodes are increased with an error smaller than 1.8 dB in amplitude and 0.25% in frequency. However, in case of amplitude reductions, the measured amplitude variations are smaller than the expected values. The error reaches 6 dB when the desired variation is −10 dB.

4.3. Modifications of first frequency

The second experiment aims at changing the frequency of the first peak without modifying its amplitude. The frequencies assigned to the first peak are less than that of the spurious peak, initially located in 529.7 Hz (Figure 5b) in order to minimize its modifications. The desired frequency variations are −5.6%, −2.8%, +2.9% and +5.9%, so that the pitch of the note is modified by −1/2 tone, −1/4 tone, +1/4 tone and +1/2 tone. To find the controller coefficients, we measure the open-loop transfer function $G_2 K \mathrm{e}^{-2\mathrm{j}\pi f \tau_{\mathrm{DSP}}} H_{\mathrm{corr}}$ using the block diagram of Figure 5a.

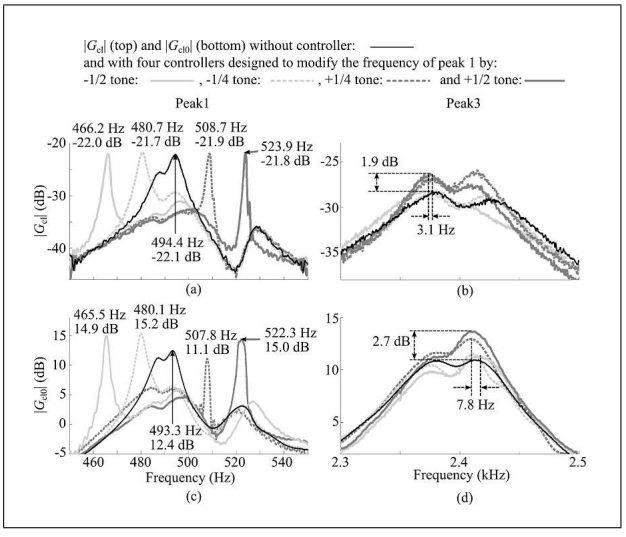

Figure 10. Closed-loop transfer functions G_{cl}, (a) and (b), and G_{cl0}, (c) and (d), measured with four different controllers designed to modify the first peak frequency, (a) and (c), by $-1/2$ tone, $-1/4$ tone, $+1/4$ tone and $+1/2$ tone, without changing the third peak, (b) and (d). The rest of the transfer function (not shown in the figure) is not modified.

Table IV. Coefficients of controllers designed to modify the first peak frequency by $-1/2$ tone, $-1/4$ tone, $+1/4$ tone and $+1/2$ tone. H_1 assigns the desired amplitude at the desired frequency, while H_1' aims at reducing the initial peak of the closed-loop transfer function. H_1' is only used when the peak frequency is increased. N_{s1} and N_{s1}' are the buffers' lengths associated to the filters H_1 and H_1'. They set the phase coefficients of the controllers.

		-1/2 tone	-1/4 tone	+1/4 tone	+1/2 tone
H_1	$H_{\max_1}$	153	54	124	142
	f_{c1}	466.7	480.3	508.9	523.8
	Q_{c1}	29	29	100	50
	N_{s1}	66	62	27	35
H_1'	$H'_{\max_1}$	not relevant		-51	-51
	f'_{c1}			494.4	494.4
	Q'_{c1}			4	4
	N'_{s1}			37	37

The curves of G_{cl}, shown in Figures 10a and 10b, are measured with a spectrum analyser using the experimental setup of Figure 2, and then are smoothed using a Savitzky-Golay filter of order 15, which does not change the frequency and amplitude of the peaks significantly.

This experiment was carried out two days after the previous one. Variations of room temperature and relative humidity slightly modified the first peak characteristics compared to measurements shown in Figure 9a; by 3.5 cents in frequency and 0.2 dB in amplitude. The controller coefficients are given in Table IV.

For each controller, the filter H_1 is centred on the desired frequency. Its bandwidth must be large enough to attenuate the closed-loop gain at the initial frequency, equal to 494.4 Hz. When the frequency is decreased, the value assigned to the Q-factor is set to 29. Smaller values would induce significant modifications on the subsequent peak of initial frequency 529.7 Hz. For this reason, as the desired frequency gets closer to 529.7 Hz, the Q-factor is increased. Consequently the closed-loop gain is less attenuated at the initial peak frequency. In order to impose a larger reduction, a second filter H_1' with negative coefficient $H'_{\max_1}$ is used to attenuate the initial peak in 494.4 Hz.

With each controller, the measured variations of the peaks of G_{c1} differ from the desired ones by less than 0.1% in frequency and 0.4 dB in amplitude. As expected, the bandwidth of the considered peak decreases as the frequency variation increases in absolute value. Smaller values of Q_{c1} compensate for this bandwidth reduction but increase the errors in amplitude and frequency. During these experiments, the third peak characteristics are subjected to small frequency and amplitude variations, less than 0.13% (3.1 Hz) and 1.9 dB, not audible according to Fastl and Zwicker [20].

The transfer functions G_{cl0} obtained with each controller are displayed in Figures 10c and 10d. The relative error between the measured and the desired frequency of the first peak is less than 0.2%. The largest variations observed on the third peak, less than (7.8 Hz) in frequency and 2.7 dB in amplitude, are hardly audible according to Fastl and Zwicker [20]. However the amplitude variations of the first peak are much larger than those of G_{cl}, especially for large frequency variations.

To get frequency variations larger than one semi-tone, higher values of $H_{\max_1}$ are required. Then a larger amplifier gain is necessary to provide the actuators with the required voltage.

In this experiment, the controllers apply frequency variations between $-1/2$ tone and $+1/2$ tone to the first peak of the closed-loop transfer function. Its amplitude variation remains below 0.4 dB. When the bar is impacted by a hammer at its centre, the measured frequency variations differ from the expected values by less than 0.2%. However the peak amplitude is subject to larger errors, up to 2.8 dB.

4.4. Simultaneous modifications of frequencies and amplitudes

In this experiment two controllers are used to modify the tuning of the xylophone bar in composite. The first is intended to move the third peak to the nominal frequency of D7 and the second to the nominal frequency of E♭7, i.e. 2349 Hz and 2489 Hz respectively, using A440 tuning in equal temperament. Thus the musical interval between partials 1 and 3 is approximately two octaves and one minor third in the first case, and two octaves and one major third in the second. The controllers also increase the level of the first and the third peaks by 7.5 dB and 10 dB respectively. They are composed of two filters whose coefficients are given in Table V.

For each controller, the closed-loop transfer function $G_{\mathrm{cl}} = Y/U_2|_{F_h=0}$ is measured with a spectrum analyser

Table V. Coefficients of controllers designed to modify simultaneously the amplitudes of peaks 1 and 3 (by 7.5 dB and 10 dB) and to move the frequency of peak 3 (to 2349 Hz and 2489 Hz). N_{s1} and N_{s3} are the buffers' lengths associated to the filters H_1 and H_3. They set the phase coefficients of the controllers.

		2349 Hz	2489 Hz
H_1	$H_{\max_1}$	16	16
	f_{c1}	494.5	494.5
	Q_{c1}	100	100
	N_{s1}	37	37
H_3	$H_{\max_3}$	16	33
	f_{c3}	2349.0	2489.0
	Q_{c3}	100	100
	N_{s3}	16	7

using the experimental setup of Figure 2. The curves are smoothed using a Savitzky-Golay filter of order 15, which does not change the frequency and the amplitude of the peaks significantly (Figures 11a and b). Each controller assigns the desired frequency variations with no significant error (less than 1.5 cent). The difference between the measured amplitudes and the desired values are less than 0.2 dB for the first peak and 0.7 dB for the third peak.

For each controller, the closed-loop transfer function $G_{\mathrm{cl0}} = Y/F_h|_{U_2=0}$ is measured using the impact hammer and the experimental setup described in §3.1.1. The measured curves of magnitude and phase are plotted in Figures 11c and 11d. In each case, the third resonance frequencies of G_{cl0} and G_{cl} differ by less than 1 Hz. Also the first peak frequency is changed by less than 0.3 Hz compared to its initial value without controller. The differences between the desired amplitudes and the measured values are less than 1.7 dB for the first peak and 1.0 dB for the third peak. Thus these errors have the same order of magnitude as the ones previously measured on G_{cl}.

Finally the system without controller and then with each of both controllers is excited four times by using a mallet. In order to compare the amplitude and frequency variations of the peaks to those measured in G_{cl0}, the impact is applied at the same position as the impact of the hammer, i.e. at the centre of the xylophone bar. The radiated sound is recorded in an arbitrary position in the near-field of the bar. The microphone is located 20 cm away from the impact point, forms an angle of 60° with the axis perpendicular to the upper face of the bar in its centre, and an azimuth of 0° with the bar axis.

For each configuration (without controller, with first controller and with second controller), the four waveforms are normalised so that their maximum value is 1, and their spectra are calculated with a frequency resolution of 0.1 Hz. The standard deviations of the peaks' frequencies are less than 0.15 cents for the first peak, and 0.8 cents for the second and third peaks. The maximum deviation is always reached in the absence of controller. The standard deviations of the peaks' amplitudes are less than 0.3 dB, 0.2 dB and 0.5 dB for the first, the second and the third

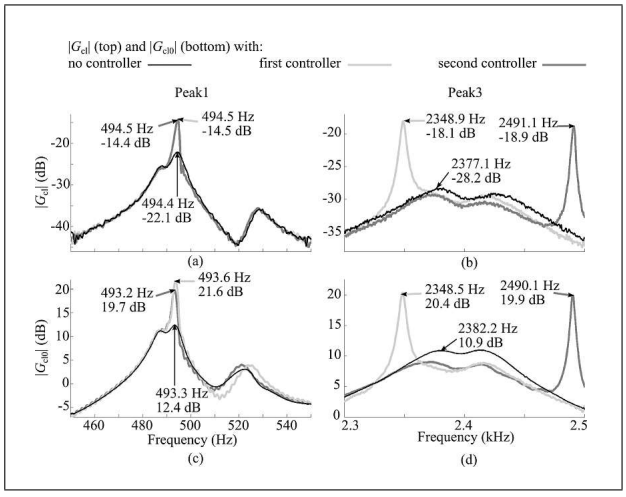

Figure 11. Closed-loop transfer functions G_{cl}, (a) and (b), and G_{cl0}, (c) and (d), with no controller (solid black), and then with two different controllers: the first (pale grey) is intended to decrease the third peak frequency to 2349 Hz, nominal frequency of D7, and the second (dark grey) to increase it to 2489 Hz, nominal frequency of E♭7, as shown in (b) and (d). They both aim at adding 7.5 dB to the first peak and 10 dB to the third peak. The rest of the transfer function (not shown in the figure) is not modified.

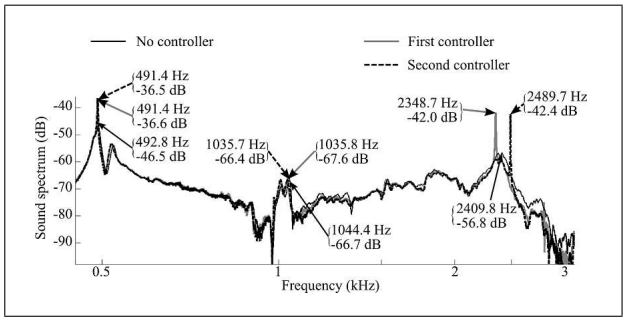

Figure 12. Sound spectrum recorded 20 cm away from centre of xylophone bar with no controller (solid black) and with two different controllers: the first (grey) is designed to decrease the third peak frequency to 2349 Hz and the second (dashed black) to increase it to 2489 Hz. They both aim at adding 7.5 dB to the first peak and 10 dB to the third peak. The curves are plotted as a function of the frequency displayed on a logarithmic scale.

peak respectively. These values show that the characteristics of the first three peaks are highly repeatable. Figure 12 shows the spectra of the average waveforms, and the amplitudes and frequencies of these peaks.

Both controllers slightly reduce the fundamental frequency of the recorded sound by a hardly audible variation, less than 0.3% i.e. about 5 cents. With each controller, the frequency difference between the third partial and the desired value, less than 0.03%, is not significant.

The peak amplitudes differ from the expected values by 2.4 and 2.5 dB for the fundamental and by 4.8 and 4.4 dB for the third partial. These errors are very sensitive to the position of the impact and the microphone. Indeed in the radiated sound, the relative difference of level between the partials has strong angular dependence.

In this experiment, the controllers have modified the tuning of the xylophone bar: the frequency separation between the first and the third partials has been consecutively set to two octaves and one minor third and two octaves and one major third. The sustain of these partials has also been extended by increasing the amplitude of the first and third peaks of the closed loop transfer function by 7.5 dB and 10 dB. The sound samples are available on the LAM website [21].

5. Conclusion

In this paper we have described a simple method of active control that can enhance the acoustic possibilities of a xylophone bar made of composite material. It uses mid-range DSP and amplifier, with regular specifications. It only requires one pair of transducers – two actuators supplied with the same voltage and one sensor – the positions of which were adjusted to not disturb the performer.

The active control method designs controllers composed of second order band-pass filters. Each filter is used to modify the frequency and amplitude of one resonance of the system.

Such controllers were applied to a simple model of a xylophone bar. They achieved independent variations of frequency and amplitude on the first resonance peak. Modifications of the controller's Q-factor also induced changes on the peak bandwidth.

The stability of the closed-loop system was investigated using the Routh-Hurwitz criterion. In general, it does not give analytic conditions on the controller coefficients. However it is helpful to test if the closed-loop system is stable with a given controller. In practice, the performer can also determine controller coefficients for which the system is stable through a preliminary calibration step.

The method was illustrated by decreasing and increasing the first and third resonance peaks of the xylophone bar by up to 10 dB and the first peak frequency by up to one semi-tone. It was then used to modify the tuning of the xylophone bar.

This active control technique offers several significant interesting possibilities to the performers. First it allows him to modify the frequency and the relative level of the partials in the radiated sound. Thus it provides the performer with a new musical instrument whose possibilities are increased. In addition, the performer can adjust the degree of modification applied by the controller to the resonances of the structure. In consequence, with such a method, he keeps his playing technique unchanged when no controller is applied and gradually adapts it as the extent of modification increases.

This method can be applied to the vibrating structure of other musical instruments and may also help to investigate their sound quality.

References

[1] C. Besnainou: Modal stimulation: a sound synthesis new approach. Proc. International Symposium on Musical Acoustics ISMA 95, Dourdan, France, 1995, 434–438.

[2] C. Besnainou: Transforming the voice of musical instruments by active control of the sound radiation. Proc. International Symposium on Active Control of Sound and Vibration ACTIVE 99, Fort Lauderdale, USA, 1999, 1317–1321.

[3] R. Chollet, G. Aeberli, C. Besnainou: Modification de la résonance de Helmholtz de la guitare par contrôle actif. Actes du 5ème Congrès Français d'Acoustique CFA 00, Lausanne, Suisse, 2000, 248–250.

[4] H. Boutin, C. Besnainou: Physical parameters of the violin bridge changed by active control. J. Acoust. Soc. Am. **123** (2008) 3656.

[5] H. Boutin, C. Besnainou: Physical parameters of an oscillator changed by active control: application to a xylophone bar. Proc. 11th International Conference on Digital Audio Effects DAFX 08, Espoo, Finland, 2008, 173–176.

[6] E. Berdahl, J. O. Smith: Active damping of a vibrating string. Proc. International Symposium on Active Control of Sound and Vibration ACTIVE 2006, Adelaide, Australia, 2006.

[7] E. Berdahl, J. O. Smith: Inducing unusual dynamics in acoustic musical instruments. Proc. International Conference on Control Applications CCA 2007, Singapore, 2007, 1336–1341.

[8] A. McPherson: The magnetic resonator piano: Electronic augmentation of an acoustic grand piano. J. New Music Res. **39** (2010) 189–202.

[9] J. D. Rollow: Active control of spectral detail radiated by an air-loaded impacted membrane. PhD thesis, Pennsylvania State University, 2003.

[10] M. Lupone, L. Seno: Gran cassa and the adaptive instrument feed-drum. – In: Computer Music Modeling and Retrieval. Springer, Berlin, Heidelberg, 2006, 149–163.

[11] M. Van Walstijn, P. Rebelo: The prosthetic conga: towards an actively controlled hybrid musical instrument. Proc. International Computer Music Conference, Barcelona, Spain, 2005, 786–789.

[12] I. Bork: Practical tuning of xylophone bars and resonators. Appl. Acoust. **46** (1995) 103–127.

[13] A. Chaigne, V. Doutaut: Numerical simulations of xylophones. I. Time-domain modeling of the vibrating bars. J. Acoust. Soc. Am. **101** (1997) 539–557.

[14] A. Chaigne, M. Bertagnolio, C. Besnainou: Tuning of xylophone bars: influence of curvature and inhomogeneities. Proc. International Symposium on Musical Acoustics ISMA 01, Perugia, Italia, 2001, 2, 531–534.

[15] N. H. Fletcher, T. D. Rossing: The physics of musical instruments. Springer-Verlag, New York Inc., 1988. chapter 19.3, Tuning the Bars, 539-542.

[16] B. H. Suits: Basic physics of xylophone and marimba bars. Am. J. Phys. **69** (2001) 743–750.

[17] H. Boutin: Méthodes de contrôle actif d'instruments de musique: cas de la lame de xylophone et du violon. PhD thesis, Université Pierre et Marie Curie, 2011.

[18] H. H. Hwang, P. C. Tripathi: Generalisation of the Routh-Hurwitz criterion and its applications. Electron. Lett. **6** (1970) 410–411.

[19] A. Savitzky, M. J. E. Golay: Smoothing and differentiation of data by simplified least squares procedures. Analytical Chemistry **36** (1964) 1627–1639.

[20] H. Fastl, E. Zwicker: Psychoacoustics: facts and models. Springer-Verlag, Berlin, 2001.

[21] Website of LAM, Institut d'Alembert UPMC Univ. Paris 6. http://www.lam.jussieu.fr/Membres/Boutin/sons.html, 2011.